Deterministic generation of maximally discordant mixed states by dissipation

X. X. Li, H. D. Yin,* D. X. Li, and X. Q. Shao†

Center for Quantum Sciences and School of Physics, Northeast Normal University, Changchun 130024, China and Center for Advanced Optoelectronic Functional Materials Research, and Key Laboratory for UV Light-Emitting Materials and Technology of Ministry of Education, Northeast Normal University, Changchun 130024, China

(Received 20 May 2019; revised manuscript received 15 November 2019; published 17 January 2020)

Entanglement can be considered as a special quantum correlation, but not the only kind. Even for a separable quantum system, nonclassical correlations are allowed to exist. Here we propose two dissipative schemes for generating a maximally correlated state of two qubits in the absence of quantum entanglement, which was proposed by Galve *et al.* [F. Galve, G. L. Giorgi, and R. Zambrini, Phys. Rev. A **83**, 012102 (2011)]. These protocols take full advantage of the interaction between four-level atoms and strongly lossy optical cavities. In the first scenario, we alternatively change the phases of two classical driving fields, while the second proposal introduces a strongly lossy coupled-cavity system. Both schemes can realize all Lindblad terms required by the dissipative dynamics, guaranteeing the maximally quantum dissonant state to be the unique steady state for a certain subspace of the system. Moreover, since the target state is a mixed state, the performance of our method is evaluated by the definition of superfidelity $G(\rho_1, \rho_2)$, and the strictly numerical simulations indicate that fidelity outstripping 99% of the quantum dissonant state is achievable with the current cavity quantum electrodynamics parameters.

DOI: 10.1103/PhysRevA.101.012329

I. INTRODUCTION

As one of the most striking features in quantum theory, quantum entanglement is recognized as the essential resource for quantum information processing [1]. For instance, it is widely used in quantum key distribution [2], superdense coding [3], quantum teleportation [4], and quantum computation [5]. Theoretically, maximally entangled states (like Bell states) have the best performance in the above tasks. However, in reality, the decoherence effect due to the environment makes the pure entangled state into a statistical mixture and degrades quantum entanglement. It is natural to ask whether the mixed state is useful for quantum information or not. The answer is positive; for example, the Werner state is a typical mixed state, which is defined by a class of two-body quantum mixtures. It has many features like invariance under the unitary transformation [6], which has been used in the description of noisy quantum channels, such as nonadditivity claims and the study of deterministic purification [7].

Quantum discord, a measure of the total quantum correlations, is defined as the difference between the quantum mutual information and the classical correlations at the quantum level [8]. It attempts to quantify all quantum correlations including entanglement. The study of quantum discord has a crucial importance for the full development of new quantum technology because it is more robust than entanglement against the effects of decoherence [9,10]. Discord between bipartite systems can be consumed to encode information with some constraints on measurement. Researchers have experimentally encoded information within the discordant correlations of two separable Gaussian states to use discord as a physical resource [11]. Especially, Galve *et al.* found some mixed states have greater values of quantum discord than pure states [12], and they identified the family of mixed states which maximize the discord for a given value of the classical correlations. On the basis of this work, López *et al.* mathematically described a method to produce the maximally correlated states without entanglement [13] and gave an example of the unitary dynamic process, which restricts the evolution time of the system.

The quantum dissipation characterized by a Lindblad generator in Markovian quantum master equations originates from the weak coupling between quantum systems and environment. Traditionally, it has been considered as a detrimental effect on quantum information processing. Nevertheless, appearances of various dissipative schemes show that the environment can be used as a resource for quantum computation and entanglement generation [14–30]. In particular, Kastoryano *et al.* [17] have discussed how to prepare highly entangled states via the loss of photons from an optical cavity. In Ref. [19], the authors proposed a dissipative scheme to generate maximal entanglement between two Rydberg atoms, where the spontaneous emissions of atoms play a positive role. Dalla Torre *et al.* presented and analyzed a new approach for the generation of atomic spin-squeezed states using the interaction between four-level atoms and a single-mode cavity [31].

Enlightened by the work of Ref. [31], we construct two physical models by taking the environment as a resource to generate the maximally discordant mixed state. This approach has the following advantages.

(i) Compared with the unitary dynamic evolution, the dissipative process is independent of time.

*yinhd239@nenu.edu.cn
†shaoxq644@nenu.edu.cn

(ii) The initial state is not strictly required by both schemes, and the target state can be successfully prepared as long as the state $|\Psi^-\rangle = (|01\rangle - |10\rangle)/\sqrt{2}$ is not populated initially.

(iii) The investigated systems make full use of the cavity decay rate κ while the spontaneous emission rates γ of atoms are suppressed. Therefore, the parameters κ and γ are permitted to have a wide range of values to improve the experimental feasibility.

The remainder of the paper is organized as follows. In Sec. II, we briefly review the properties of maximally discordant mixed states. In Sec. III, we construct one physical model with a pair of four-level atoms trapped in a strongly lossy optical cavity. Under the large decay of the cavity and alternatively changing the Rabi frequencies of classical fields, we derive an effective master equation and numerically simulate the effects of relevant parameters on the prepared state. In Sec. IV, we introduce another physical model which requires a coupled cavity with atoms separately trapped in each cavity. In Secs. V and VI we discuss the potential experimental feasibility and give a brief summary of the paper, respectively.

II. BRIEF REVIEW OF THE MAXIMALLY DISCORDANT MIXED STATES

The states we are interested in are found within the set of separable states. It has been shown that the most nonclassical two-qubit states, i.e., the family with maximal quantum discord versus classical correlations, were formed by mixed states of rank 2 and 3, which are named maximally discordant mixed states (MDMSs). The class of states of rank 3 is defined by [12]

$$\rho = \epsilon|\Phi^+\rangle\langle\Phi^+| + (1-\epsilon)[x|01\rangle\langle 01| + (1-x)|10\rangle\langle 10|], \quad (1)$$

where $|\Phi^+\rangle = (|00\rangle + |11\rangle)/\sqrt{2}$.

Quantum discord is defined as $I - C$, where $I = S(\rho_A) + S(\rho_B) - S(\rho_{AB})$ is quantum mutual information, where $S(\rho)$ is the von Neumann entropy and $C(\rho_{AB}) = \max\{S(\rho_A) - S(\rho_{A|B})\}$ is the classical correlation where $S(\rho_{A|B})$ is the conditional entropy of A given a measurement on the system B. Referring to the Ali-Rau-Alber results of the conditional entropy [32], the quantum mutual information is maximized when $x = 1/2$ and $\epsilon = 1/3$, while the classical correlation is minimized, which corresponds to a maximally discordant mixed state. By exchanging the basis vector $|0\rangle \leftrightarrow |1\rangle$ of the second qubit, we obtain the state in the form

$$\rho = \tfrac{1}{3}(|\Psi^+\rangle\langle\Psi^+| + |00\rangle\langle 00| + |11\rangle\langle 11|), \quad (2)$$

where $|\Psi^+\rangle = (|01\rangle + |10\rangle)/\sqrt{2}$.

Using the basis of Bell states $|\Phi^\pm\rangle = (|00\rangle \pm |11\rangle)/\sqrt{2}$ and $|\Psi^\pm\rangle = (|01\rangle \pm |10\rangle)/\sqrt{2}$ [13], the above state can be rewritten as

$$\rho = \tfrac{1}{3}(|\Phi^+\rangle\langle\Phi^+| + |\Phi^-\rangle\langle\Phi^-| + |\Psi^+\rangle\langle\Psi^+|). \quad (3)$$

When we have a system characterized by the following master equation,

$$\dot{\rho} = \mathscr{L}_{\gamma_x}[S_x]\rho + \mathscr{L}_{\gamma_y}[S_y]\rho, \quad (4)$$

where $S_x = (\sigma_x^1 + \sigma_x^2)$ and $S_y = (\sigma_y^1 + \sigma_y^2)$ ($\sigma_{x,y}$ are Pauli operators), and $\mathscr{L}_{\gamma_i}[O]\rho$ is the Lindblad term defined as $\mathscr{L}_{\gamma_i}[O]\rho = \gamma_i/2(2O\rho O^\dagger - O^\dagger O\rho - \rho O^\dagger O)$, $(i = x, y)$, the state described by Eq. (3) will be the steady state of this system. However, it is difficult to find a natural system with the above form of the master equation. Thus, we consider the design of a physical model which is equivalent to Eq. (4) under the appropriate approximations, and we will discuss our method in detail in the next section.

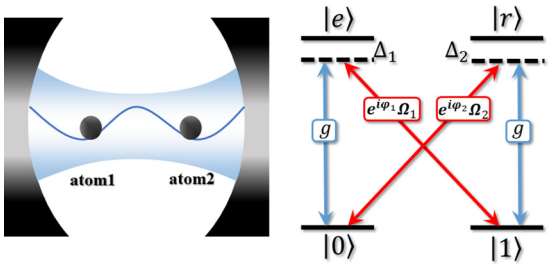

FIG. 1. Schematic view of the system and the configuration of the atoms. (a) The system consists of two atoms collectively interacting with a lossy cavity. (b) Level structure of a four-level atom which is simultaneously driven by two classical fields and coupled to a cavity mode.

III. TWO FOUR-LEVEL ATOMS IN A LOSSY CAVITY

The central idea of our paper can be understood by considering a pair of atoms interacting with a strongly lossy optical cavity, as depicted in Fig. 1. The atoms are driven by the laser fields with complex Rabi frequencies $\Omega_{1(2)}e^{i\varphi_{1(2)}}$, where $\varphi_{1(2)}$ is the phase of the classical field, and simultaneously coupled to the quantized field with strength g. The Hamiltonian in the Schrödinger picture can be written as ($\hbar = 1$)

$$\begin{aligned} H_s &= H_0 + V_s, \quad (5)\\ H_0 &= \sum_{i=1}^{2} \omega_0|0\rangle_i\langle 0| + \omega_1|1\rangle_i\langle 1| + \omega_e|e\rangle_i\langle e| \\ &\quad + \omega_r|r\rangle_i\langle r| + \nu a^\dagger a, \\ V_s &= \sum_{i=1}^{2} g(|e\rangle_i\langle 0| + |r\rangle_i\langle 1|)a + \Omega_1 e^{i\varphi_1}|e\rangle_i\langle 1|e^{-i\mu_1 t} \\ &\quad + \Omega_2 e^{i\varphi_2}|r\rangle_i\langle 0|e^{-i\mu_2 t} + \text{H.c.}, \end{aligned}$$

where ω_0, ω_1, ω_e, and ω_r are the eigenfrequencies of the lower states $|0\rangle$, $|1\rangle$ and upper states $|e\rangle$, $|r\rangle$, respectively, while ν and $\mu_{1(2)}$ are the frequencies of quantum and classical fields. $a^\dagger$ and a are the creation and annihilation operators of the optical cavity mode. In addition, the ground-state transition is dipole forbidden. For simplicity, we assume all parameters are real. In the interaction picture, the Hamiltonian of the system reads

$$\begin{aligned} H_I &= H_1 + H_2, \\ H_1 &= \sum_{i=1}^{2} ga|e\rangle_i\langle 0|e^{i\delta_1 t} + \Omega_1 e^{i\varphi_1}|e\rangle_i\langle 1|e^{i\delta_2 t} + \text{H.c.}, \\ H_2 &= \sum_{i=1}^{2} ga|r\rangle_i\langle 1|e^{i\delta_1' t} + \Omega_2 e^{i\varphi_2}|r\rangle_i\langle 0|e^{i\delta_2' t} + \text{H.c.}, \quad (6) \end{aligned}$$

where $\delta_{1(2)} = \omega_e - \omega_{0(1)} - \nu(\mu_1)$ and $\delta'_{1(2)} = \omega_r - \omega_{1(0)} - \nu(\mu_2)$. We further suppose $\delta_1 = \delta_2 = \Delta_1$ and $\delta'_1 = \delta'_2 = \Delta_2$. Now we consider the process of constructing the collective decay operator $S_y = \sigma_y^1 + \sigma_y^2$. Taking $\Omega_1 e^{i\varphi_1} = i\Omega_1$, and $\Omega_2 e^{i\varphi_2} = -i\Omega_2$, and in the regime of large detuning $|\Delta_{1(2)}| \gg \{g, \Omega_{1(2)}\}$, we can safely eliminate the upper states $|e\rangle$ and $|r\rangle$, and then the above Hamiltonian reduces to

$$H_{\text{eff}} = H_{\text{eff}}^1 + H_{\text{eff}}^2, \tag{7}$$

where

$$H_{\text{eff}}^1 = G_1 J_- a^\dagger + \text{H.c.} + \sum_{i=1}^{2} g_{\text{eff}}^1 a^\dagger a |0\rangle_i\langle 0| + \Omega_{\text{eff}}^1 |1\rangle_i\langle 1|,$$

$$H_{\text{eff}}^2 = G_2 J_+ a^\dagger + \text{H.c.} + \sum_{i=1}^{2} g_{\text{eff}}^2 a^\dagger a |1\rangle_i\langle 1| + \Omega_{\text{eff}}^2 |0\rangle_i\langle 0|,$$

with $G_{1(2)} = g\Omega_{1(2)}/\Delta_{1(2)}$, $g_{\text{eff}}^{1(2)} = -g^2/\Delta_{1(2)}$, and $\Omega_{\text{eff}}^{1(2)} = -\Omega_{1(2)}^2/\Delta_{1(2)}$. $J_+ = i(|1\rangle_1\langle 0| + |1\rangle_2\langle 0|)$ and $J_- = -i(|0\rangle_1\langle 1| + |0\rangle_2\langle 1|)$ are the collective ascending and descending operators. We further assume $G_1 = G_2 = G$, i.e., $\Omega_1/\Delta_1 = \Omega_2/\Delta_2$, and omit the Stark shifts of the ground states, and the above Hamiltonian is simplified as

$$H_{\text{eff}} = G(J_- + J_+)a^\dagger + \text{H.c.} \tag{8}$$

Since the effective system only includes the ground states, the spontaneous emissions of atoms are greatly restrained, and the master equation can be written as

$$\dot{\rho} = -i[G(J_- + J_+)a^\dagger + G(J_- + J_+)a, \rho] + \frac{\kappa}{2}(2a\rho a^\dagger - a^\dagger a\rho - \rho a^\dagger a). \tag{9}$$

In the limitation of large decay rate $\kappa \gg G$, the cavity mode can also be neglected, and we obtain the master equation characterizing the system of atoms as

$$\dot{\rho} = \mathscr{L}_{\gamma_y}[S_y]\rho, \tag{10}$$

where $\gamma_y = 4G^2/\kappa$ is the collective decay rate of the atoms.

On the other hand, if we attempt to construct the collective decay operator $S_x = \sigma_x^1 + \sigma_x^2$, we can simply take $\varphi_1 = \varphi_2 = 0$, and then after a series of similar derivations the effective master equation reads

$$\dot{\rho} = \mathscr{L}_{\gamma_x}[S_x]\rho, \tag{11}$$

where $\gamma_x = 4G^2/\kappa$, $J'_+ = |1\rangle_1\langle 0| + |1\rangle_2\langle 0|$, and $J'_- = |0\rangle_1\langle 1| + |0\rangle_2\langle 1|$.

Up to the present, we have shown how to generate the collective decay operators S_x and S_y, respectively. But the stability of Eq. (3) requires there should be $\mathscr{L}_{\gamma_x}(S_x)$ and $\mathscr{L}_{\gamma_y}(S_y)$ in the master equation at the same time. Fortunately, drawing lessons from the spin-echo effect, our model is able to simulate the effective master equation of Eq. (4) apart from a coefficient of 1/2, as long as the phases of the classical fields φ_1 and φ_2 are interchanged fast enough. The result is obtained by using the Trotter product formula (see Corollary 5.8 in Chap. 3 of Ref. [33]):

$$\lim_{N\to\infty}\left\{e^{\mathscr{L}_{\gamma_x}[S_x]\frac{T}{2N}} e^{\mathscr{L}_{\gamma_y}[S_y]\frac{T}{2N}}\right\}^N = e^{\frac{1}{2}[\mathscr{L}_{\gamma_x}[S_x] + \mathscr{L}_{\gamma_y}[S_y]]T}, \tag{12}$$

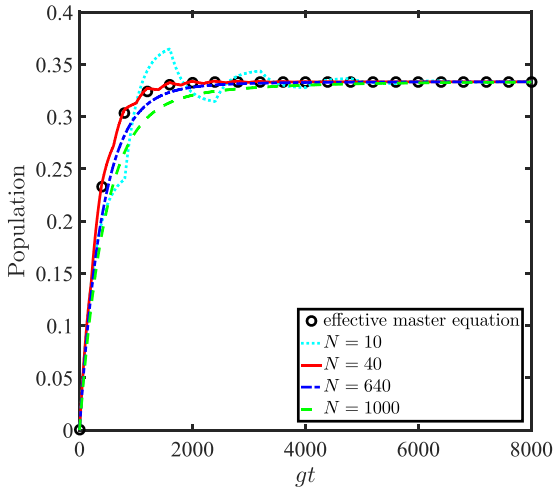

FIG. 2. The populations of $|\Psi^+\rangle$ as functions of gt governed by the effective master equation (13) and the master equations with Hamiltonian (6), where N is the switching number. The initial state is $|00\rangle|0\rangle_c$ and we set $G = 0.01$ and $\kappa = 80G$.

where T is the total evolution time. Then the effective master equation is

$$\dot{\rho} = \tfrac{1}{2}\mathscr{L}_{\gamma_x}[S_x]\rho + \tfrac{1}{2}\mathscr{L}_{\gamma_y}[S_y]\rho. \tag{13}$$

Figure 2 shows the population of $|\Psi^+\rangle$ under different evolution processes from the initial state $|00\rangle|0\rangle_c$. The evolution of the effective master equation (13) is shown with empty circles and the other lines are the switching evolutions obtained from the master equation with Hamiltonian (6). The total evolution time is $gt = 8000$. Different lines correspond to the results with different switching number N. Since we take the cavity decay as a resource for states generation, the switching number N has an upper limit promising an interval time much larger than $1/\kappa$. This can guarantee the role of κ in each process, which ensures the complete generation of the target state. In addition, the operation time $1/\gamma$ determines the minimum value of N. This ensures an interval time far less than $1/\gamma$. Thus we choose $N = 200$ and $gt = 8000$ in the following simulations if there is no special description.

In quantum information theory, distinguishing two quantum states is a fundamental task. One of the main tools used in distinguishability theory is quantum fidelity [34,35], which is widely used and has been found applications in solving problems like quantifying entanglement [36,37], quantum error correction [38], quantum chaos [39], and so on. In order to measure the distance between quantum states including mixed states, we here adopt the definition of superfidelity [40]

$$G(\rho, \sigma) = \text{Tr}[\rho(t)\sigma] + \sqrt{[1 - \text{Tr}\rho(t)^2](1 - \text{Tr}\sigma^2)}, \tag{14}$$

with σ being the density operator of the target state as $\sigma = (|\Psi^+\rangle\langle\Psi^+| + |00\rangle\langle 00| + |11\rangle\langle 11|)/3$. We initialize the system into state $|00\rangle|0\rangle_c$ and plot the fidelity of the target state under the switching evolution of the master equations with full Hamiltonian (6). Figures 3(a)–3(c), respectively, illustrate the effects of parameters κ, γ, and Ω on the preparation of the target state. Figure 3(a) shows the fidelity as a function of the cavity decay rate κ with parameters

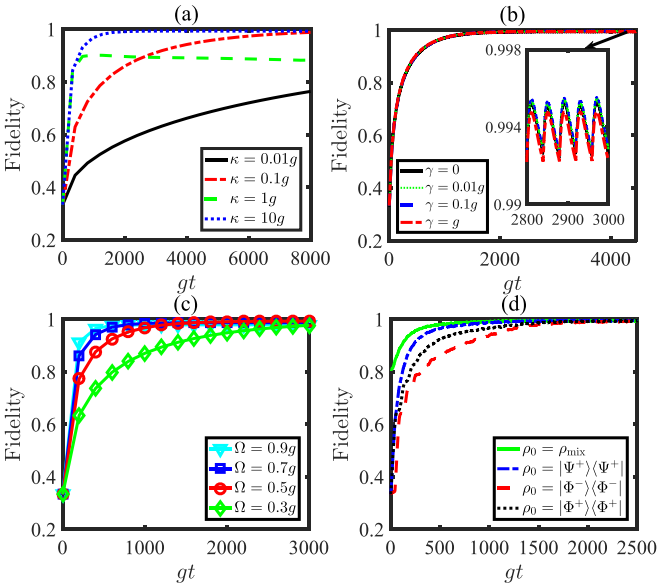

FIG. 3. The target state fidelities as functions of gt governed by the full master equation and the switching number $N = 200$. (a) Time evolutions with different cavity decay rates $\kappa = (0.01, 0.1, 1, 10)g$, where we set $\Delta_{1,2} = 100g$ and $\Omega_{1(2)} = 0.5g$. (b) Effects of atom spontaneous emission rates γ with the same parameters as in panel (a) and $\kappa = 0.1g$. The inset shows the enlarged view of the part indicated by the arrow. (c) The effects of Rabi frequencies on the target state with $\gamma = 0.1g$ and $\kappa = 0.1g$. (d) Time evolutions with different initial states, where $|\Phi^{\pm}\rangle = (|00\rangle|0\rangle_c \pm |11\rangle|0\rangle_c)/\sqrt{2}$, $|\Psi^+\rangle = (|01\rangle|0\rangle_c + |10\rangle|0\rangle_c)/\sqrt{2}$, and $\rho_{\rm mix} = (0.1|\Phi^+\rangle\langle\Phi^+| + 0.1|\Phi^-\rangle\langle\Phi^-| + 0.8|\Psi^+\rangle\langle\Psi^+|) \otimes |0\rangle_c\langle 0|$.

$\Delta_{1,2} = 100g$ and $\Omega_{1,2} = 0.5g$. The increase of κ will prolong the convergence time. This can be explained by Eqs. (9) and (10). To obtain the target state, the collective decay rate $4G^2/\kappa$ will increase as κ decreases, which results in a short convergence time. But if κ is too small, it will destroy the condition $\kappa \gg G$ and fail to generate the target state.

In Fig. 3(b), we take into account the spontaneous emissions of the atoms and plot the evolutions of the target state with different γ. Even if γ is extremely large ($\gamma \sim g$), the fidelity is still above 99%, which demonstrates that our scheme has favorable resistance to atomic spontaneous emission. The inset picture of Fig. 3(b) is the enlarged view of the part indicated by the arrow, which shows that the population keeps oscillating at the final time with small amplitude and stays around a definite value.

Moreover, the convergence time is related to the intensity of the classical field $\Omega_{1(2)}$. Figure 3(c) displays the evolution curves under different Ω with $\gamma = 0.1g$ and illustrates the optimal parameter range of the Rabi frequency. The figure shows that the optimal range of Ω is about $0.3g$–$0.7g$, which could ensure a fidelity over 99%. Figure 3(d) additionally includes the request to the initial state of the system. We can obtain the target state with arbitrary initial state except for the singlet state $|\Psi^-\rangle$.

To expound the properties peculiar to the target state, we plot the concurrence [41], classical correlation, and quantum discord of the state with the full master equation

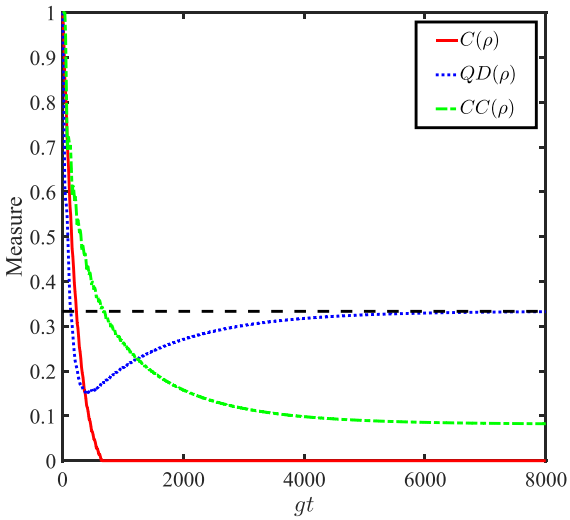

FIG. 4. The properties of the target state, which consists of the concurrence (C), classical correlation (CC), and quantum discord (QD). The initial state is $|\Psi^+\rangle$ and the black dashed line labels the number $1/3$.

in Fig. 4. It is worth mentioning that we directly utilize the results given in Ref. [42] to measure quantum discord (QD), and the calculation of $S(\rho_{A|B})$ is based on the positive-operator-valued measurements locally performed on the subsystem B. The QD and the classical correlation (CC) are given as $\mathrm{QD}(\rho) = \mathbf{min}\{Q_1, Q_2\}$ and $\mathrm{CC}(\rho) = \mathbf{max}\{\mathrm{CC}_1, \mathrm{CC}_2\}$, where $\mathrm{CC}_j = h[\rho_{11} + \rho_{22}] - D_j$ and $Q_j = h[\rho_{11} + \rho_{33}] + \sum_{k=1}^{4} \lambda_k \log_2 \lambda_k + D_j$, with λ_k being the eigenvalues of ρ and $h[x]$ being the binary entropy defined as $h[x] = -x\log_2 x - (1-x)\log_2(1-x)$. $D_1 = h[\tau]$, where $\tau = \{1 + \sqrt{[1 - 2(\rho_{33} + \rho_{44})]^2 + 4(|\rho_{14}| + |\rho_{23}|)^2}\}/2$ and $D_2 = -\sum_{k=1}^{4} \rho_{kk} \log_2 \rho_{kk} - h[\rho_{11} + \rho_{33}]$. Based on Fig. 4, the final state has the maximally quantum discord $1/3$ without entanglement and the classical relation reaches the minimum. The steady state is a maximally discordant mixed state.

Figure 5 discusses the effect of the switching number N, where the increasing of N smooths the evolution process. It also illustrates that a high fidelity over 98% can be obtained with a wide range of values for N. Even if $N = 4$ the fidelity can still get over 99%. Thus, in actual operations, we can properly reduce the value of N to simplify the experiment.

IV. TWO ATOMS IN A LOSSY COUPLED-CAVITY SYSTEM

The coupled-cavity systems are especially useful in distributed quantum computation [43–47], which is able to overcome the problem of individual addressability. The lossy coupled-cavity system in our model is shown in Fig. 6. It consists of two coupled cavities which, respectively, trap a four-level atom with ground states $|0\rangle, |1\rangle$ and excited states $|e\rangle, |r\rangle$. The transition between $|0\rangle$ ($|1\rangle$) and $|e\rangle$ ($|r\rangle$) is coupled resonantly to the quantum field with coupling constant g, and other nonresonant transitions with detuning $\pm\Delta$ are driven by classical fields with Rabi frequencies $\pm i\Omega_{1(2)}$ and $\Omega'_{1(2)}$. The Hamiltonian under the Schrödinger picture can be

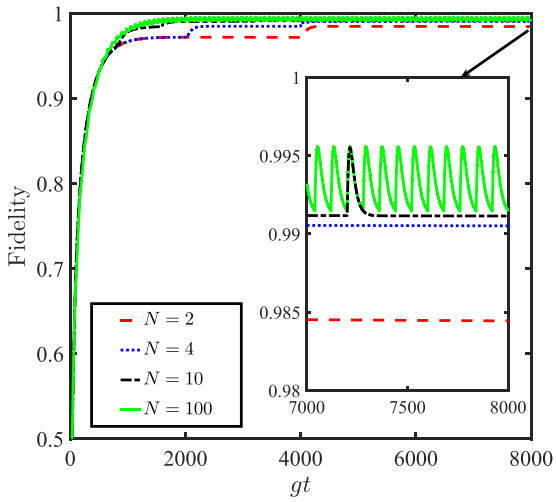

FIG. 5. Time evolution of the fidelities for the target state with different switching numbers. The initial state is $|00\rangle|0\rangle_c$. The inset shows the zoom-in fidelities from $gt = 7000$ to 8000.

written as

$$
\begin{aligned}
H &= H_0 + V_s,\\
H_0 &= \sum_{k=1}^{2} \omega_0|0\rangle_k\langle 0| + \omega_1|1\rangle_k\langle 1| + \omega_e|e\rangle_k\langle e|\\
&\quad + \omega_r|r\rangle_k\langle r| + \omega_c a_k^\dagger a_k,\\
V_s &= \sum_{k=1}^{2} g(|e\rangle_k\langle 0| + |r\rangle_k\langle 1|)a_k + \Omega_1'|e\rangle_k\langle 1|e^{-i\omega_L' t}\\
&\quad + \Omega_2'|r\rangle_k\langle 0|e^{-i\omega_L' t} + i\Omega_1(|e\rangle_1\langle 1| - |e\rangle_2\langle 1|)e^{-i\omega_L t}\\
&\quad - i\Omega_2(|r\rangle_1\langle 0| - |r\rangle_2\langle 0|)e^{-i\omega_L t} + \text{H.c.}\\
&\quad + A(a_1^\dagger a_2 + a_2^\dagger a_1),
\end{aligned}
\tag{15}
$$

where ω_i $(i = 0, 1, e, r)$ are the eigenfrequencies of ground and excited states for each atom, and ω_c is the frequency of the quantum field. $a_k^\dagger$ and a_k $(k = 1, 2)$ are creation and annihilation operators of cavity mode k, and ω_L and ω_L' are frequencies of classical fields. We switch the Hamiltonian from the Schrödinger picture to the interaction picture and

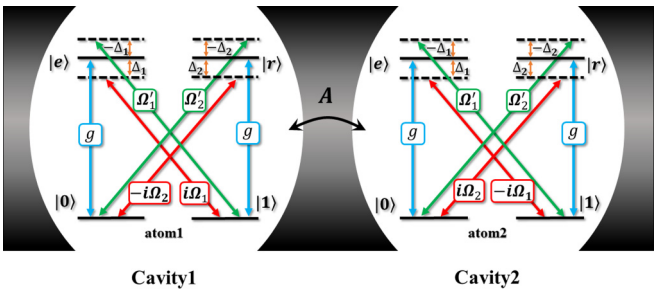

FIG. 6. Schematic view of two four-level atoms trapped in a lossy coupled-cavity array. Each atom is simultaneously driven by four classical fields with Rabi frequencies $\pm i\Omega_{1(2)}$, $\Omega'_{1(2)}$, detuned by $\pm\Delta_{1(2)}$ and resonantly coupled with the corresponding cavity mode. The photon can hop between two cavities with coupling strength A.

obtain

$$
\begin{aligned}
H_I &= \sum_{k=1}^{2} g(|e\rangle_k\langle 0| + |r\rangle_k\langle 1|)a_k + i\Omega_1 e^{i\Delta_1 t}(-1)^{k-1}|e\rangle_k\langle 1|\\
&\quad + i\Omega_2 e^{i\Delta_2 t}(-1)^k|r\rangle_k\langle 0| + \Omega_1' e^{-i\Delta_1 t}|e\rangle_k\langle 1|\\
&\quad + \Omega_2' e^{-i\Delta_2 t}|r\rangle_k\langle 0| + \text{H.c.} + A(a_1^\dagger a_2 + a_2^\dagger a_1),
\end{aligned}
\tag{16}
$$

where $\Delta_1 = \omega_e - \omega_1 - \omega_L = \omega_1 + \omega_L' - \omega_e$, $\Delta_2 = \omega_r - \omega_0 - \omega_L = \omega_0 + \omega_L' - \omega_r$, and we suppose $\Delta_1 = \Delta_2 = \Delta$. Now we introduce a pair of delocalized bosonic modes in order to remove the localized modes as follows [47]:

$$
m_1 \equiv \frac{1}{\sqrt{2}}(a_1 - a_2), \quad m_2 \equiv \frac{1}{\sqrt{2}}(a_1 + a_2). \tag{17}
$$

Then we have

$$
\begin{aligned}
H_I &= \sum_{k=1}^{2} \frac{g}{\sqrt{2}} m_1 e^{iAt}(-1)^{k-1}(|e\rangle_k\langle 0| + |r\rangle_k\langle 1|)\\
&\quad + \frac{g}{\sqrt{2}} m_2 e^{-iAt}(|e\rangle_k\langle 0| + |r\rangle_k\langle 1|) + \Omega_1' e^{-i\Delta t}|e\rangle_k\langle 1|\\
&\quad + \Omega_2' e^{-i\Delta t}|r\rangle_k\langle 0| + i\Omega_1 e^{i\Delta t}(-1)^{k-1}|e\rangle_k\langle 1|\\
&\quad + i\Omega_2 e^{i\Delta t}(-1)^k|r\rangle_k\langle 0| + \text{H.c.}
\end{aligned}
\tag{18}
$$

We set $A = \Delta$ to guarantee the two-photon resonance, and choose $\Omega_{1(2)} = \Omega'_{1(2)} = \Omega$. Under the large detuning condition, i.e., $|\Delta| \gg \{g, \Omega\}$, and neglecting the Stark-shift terms, the effective Hamiltonian reads

$$
\begin{aligned}
H_{\text{eff}} &= \sum_{k=1}^{2} \frac{g\Omega}{\sqrt{2}\Delta} m_1(-i|0\rangle_k\langle 1| + i|1\rangle_k\langle 0|)\\
&\quad + \frac{g\Omega}{\sqrt{2}\Delta} m_2(|0\rangle_k\langle 1| + |1\rangle_k\langle 0|) + \text{H.c.}
\end{aligned}
\tag{19}
$$

Based on the definition of collective decay operators $S_x = (\sigma_{1x} + \sigma_{2x})$ and $S_y = (\sigma_{1y} + \sigma_{2y})$, the effective Hamiltonian can be rewritten as

$$
H_{\text{eff}} = Gm_1 S_y + Gm_2 S_x + \text{H.c.}, \tag{20}
$$

where $G = g\Omega/\sqrt{2}\Delta$. It can be seen that the current system only involves couplings between ground states and delocalized cavity modes. Therefore, the dissipative dynamics of the system can be considered as governed by the following master equation:

$$
\dot{\rho} = i[\rho, H_{\text{eff}}] + \sum_{k=1}^{2} \frac{\kappa}{2}(2m_k\rho m_k^\dagger - m_k^\dagger m_k\rho - \rho m_k^\dagger m_k). \tag{21}
$$

In the limit $\kappa \gg |G|$, we can adiabatically eliminate the delocalized cavity modes, and obtain the effective master equation:

$$
\dot{\rho} = \mathscr{L}_{\gamma_x}[S_x]\rho + \mathscr{L}_{\gamma_y}[S_y]\rho, \tag{22}
$$

where $\gamma_x = \gamma_y = 4G^2/\kappa$. Compared with the previous model, the coupled-cavity system provides the means to realize $\mathscr{L}_{\gamma_x}[S_x]$ and $\mathscr{L}_{\gamma_y}[S_y]$ simultaneously. Thus the target state $\rho = (|\Psi^+\rangle\langle\Psi^+| + |00\rangle\langle 00| + |11\rangle\langle 11|)/3$ can be generated using the driven-dissipative dynamics.

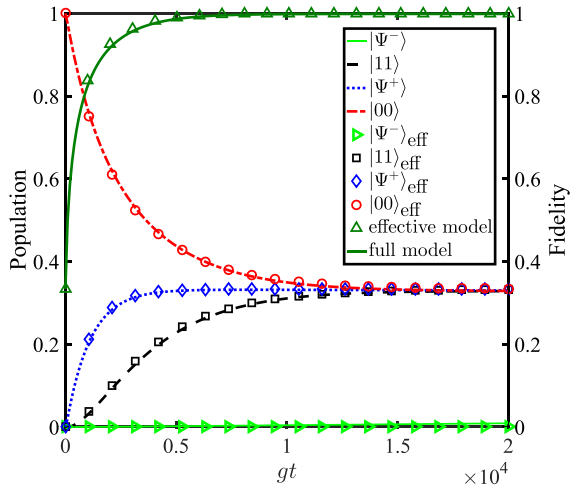

FIG. 7. Time evolution of populations (shown in the red dash-dotted line, blue dotted line, black dashed line, and green full line) and fidelities (shown in dark green) of the target state under the full and effective master equations, where $\kappa = 0.1g$, $\Omega = 0.2g$, $\Delta = 100g$, and $\gamma = 0$.

To verify the effectiveness of our scheme in generating MDMSs, we plot the population and the fidelity of the target state with the initial state $|00\rangle|00\rangle_c$ governed by the full and effective master equation in Fig. 7, respectively. We find that these two lines perfectly coincide with each other and the state prepared by our scheme can maintain a high fidelity close to unity after $gt = 10\,000$. The selections of numerical simulation parameters are $\kappa = 0.1g$, $\Omega = 0.2g$, and $\Delta = 100g$.

Then we make the same illustrations as Fig. 3 in the coupled-cavity system. The results are shown in Fig. 8, which shows similar phenomena of κ, ρ_0, γ, and Ω. Compared with the first scenario, the fidelity is higher and the final population is stable after a longer evolution time.

V. DISCUSSION

Now, we discuss the basic elements that may be candidates for the intended experiment. The possible realizations of these physical models could be set up in ^{87}Rb using the clock states $|F = 1, m_F = 0\rangle$ and $|F = 2, m_F = 0\rangle$ in the $5S_{1/2}$ ground-state manifold as two lower levels $|0\rangle$ and $|1\rangle$. In addition, the states $|F = 1, m_F = +1\rangle$ and $|F = 2, m_F = +1\rangle$ of the $5P_{1/2}$ manifold could be used as two higher levels $|e\rangle$ and $|r\rangle$ [31]. The possible realizations of these physical models are indicated in Fig. 9(a), in which we only show the couplings between two polarization-dependent lasers and the four-level atoms in the coupled-cavity system for simplicity. Figure 9(b) provides a method of the alignment of lasers. We use two pulses traveling in the y direction driving two atoms in the xz plane, respectively. Since the Rabi frequency is presented as $\Omega_{1(2)}e^{i\varphi_{1(2)}}$, which cannot be simply displayed, we only plot the imaginary part to illustrate the phase relations. Here we take xz as a reference plane (shadow area) and Ω_2' as a standard pulse the phase of which equals to zero ($\varphi_2 = 0$). The other pulses $\pm i\Omega_2$ can be obtained by modulating the initial phases $\varphi_2 = \pm\pi/2$ relative to the standard classical field. Thus, we could construct a group of pulses to meet the

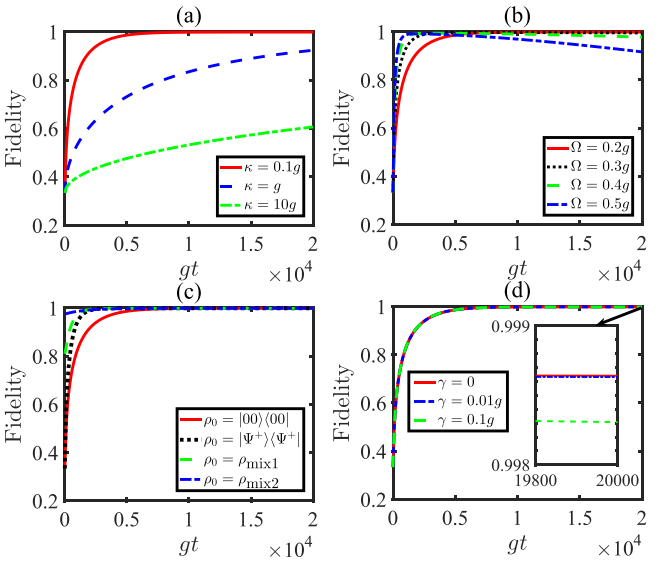

FIG. 8. Time evolutions of the target state fidelities under the full master equation with different parameters. (a) Different curves correspond to different cavity decay rates κ. The other parameters are $\Delta = 100g$ and $\Omega = 0.2g$. (b) The effects of Rabi frequencies Ω on the target state with $\kappa = 0.1g$ and the other parameters are the same as in panel (a). (c) Different evolution processes under different initial states, where $|\Psi^+\rangle = (|01\rangle|00\rangle_c + |10\rangle|00\rangle_c)/\sqrt{2}$, $\rho_{\rm mix1} = (0.1|00\rangle\langle 00| + 0.1|11\rangle\langle 11| + 0.8|\Psi^+\rangle\langle\Psi^+|) \otimes |00\rangle_c\langle 00|$, and $\rho_{\rm mix2} = (0.2|00\rangle\langle 00| + 0.5|11\rangle\langle 11| + 0.3|\Psi^+\rangle\langle\Psi^+|) \otimes |00\rangle_c\langle 00|$. (d) Atom spontaneous emission rates $\gamma = (0, 0.01, 0.1)g$. The other parameters are the same as above. The inset picture is the enlarged view of the part indicated by the arrow.

above phase conditions. Note that we only show the coupling between $|0\rangle$ and $|r\rangle$ here, while for the coupling between $|1\rangle$ and $|e\rangle$ we can do similar operations.

According to past works [48–51], the transition between the atomic ground level $5S_{1/2}$ and the optical level $5P_{1/2}$ of the ^{87}Rb atom is coupled to the quantized cavity mode with strength $g = 2\pi \times 14.4$ MHz. The spontaneous emission rate is $\gamma = 2\pi \times 3$ MHz and the cavity decay rate is $\kappa = 2\pi \times 0.66$ MHz. The Rabi frequencies $\Omega_{1,2}$ can be tuned continuously and for the first scheme we adopt parameters

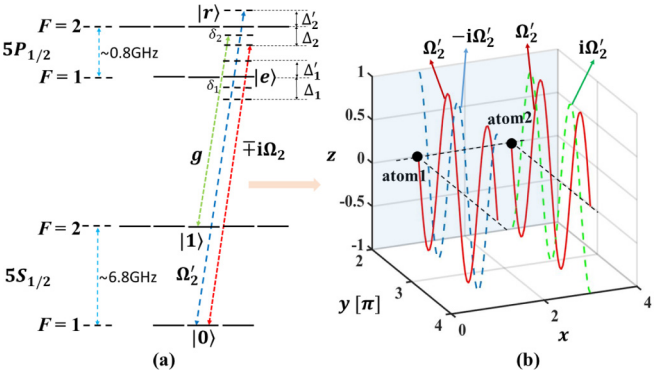

FIG. 9. Experimental level scheme in ^{87}Rb using the clock state of the second scenario. Together they show a set of phase relations matching the conditions.

$\Omega_{1,2} = 0.3g$, $\Delta_{1,2} = 76g$, and $N = 200$, and the fidelity of the target state is 99.41%. For the second one, we set $\Omega_{1,2} = \Omega'_{1,2} = 0.1g$, and $\Delta_{1,2} = 50g$, and the fidelity is 99.56%.

In addition, Ref. [52] reported the projected limits for a Fabry-Pérot cavity, where the coupling coefficient $g = 2\pi \times 770\,\mathrm{MHz}$. Based on the corresponding critical photon number and critical atom number, we obtain $(\kappa, \gamma) = 2\pi \times (21.7, 2.6)\,\mathrm{MHz}$. The fidelity F reaches 99.10% for the first scheme with the other relevant parameters selected as $\Omega_{1,2} = 0.2g$, $\Delta_{1,2} = 72g$, and $N = 200$. For the second one, the fidelity is 99.67%, while other parameters are $\Omega_{1,2} = \Omega'_{1,2} = 0.12g$ and $\Delta_{1,2} = 50g$. Moreover, in a microscopic optical resonator [53], the parameters of an atom interacting with an evanescent field are $(g, \kappa, \gamma) = 2\pi \times (70, 5, 1)\,\mathrm{MHz}$, which correspond to the fidelity $F = 99.18\%$ with parameters $\Omega_{1,2} = 0.3g$, $\Delta_{1,2} = 43g$, and $N = 200$ in the first scheme and $F = 99.34\%$ with parameters $\Omega_{1,2} = \Omega'_{1,2} = 0.1g$ and $\Delta_{1,2} = 50g$ in the second scheme.

So far, we have discussed how to prepare the MDMS on the basis of a perfect phase-matching condition $\varphi_{1(2)} = \pm 0.5\pi$. Nevertheless, the effect of phase mismatch is unavoidable in experiments. Thus it is necessary to discuss the effects caused by this error. For the sake of convenience, we suppose that the Rabi frequencies of lasers related to the collective decay operator S_x are perfect, and the phase mismatch is only introduced as executing the collective decay operator S_y, and thence the effective master equation of the first model is written as

$$\dot{\rho}_{m1} = \frac{1}{2}\mathscr{L}_\gamma\left[\sum_{k=1}^{2} -ie^{i\delta\varphi_1}|0\rangle_k\langle 1| + ie^{i\delta\varphi_2}|1\rangle_k\langle 0|\right]\rho + \frac{1}{2}\mathscr{L}_\gamma[S_x]\rho, \tag{23}$$

where $\delta\varphi_i$ denotes the phase deviation from the standard value. Figure 10(a) using the effective master equation (23) characterizes the effects of phase mismatch $\delta\varphi_{1(2)}$ on the fidelity of the first scenario from the perspective of dynamic evolution. Starting from the initial state $|00\rangle|0\rangle_c$, a high-fidelity MDMS is always attainable for a long time except $\delta\varphi_1 = -\delta\varphi_2 = \pm 0.5\pi$ (see the Appendix for detail). The above conclusion is further verified in Fig. 10(b), the evolution of which is governed by the full master equation by considering $\delta\varphi_1 = -\delta\varphi_2$. These results, in turn, show that the condition of dissipatively preparing the MDMS in Ref. [13] is not necessary. In fact, there are many combinations of collective decay operators that can realize the MDMS. For example, the target state $\rho = (|\Phi^+\rangle\langle\Phi^+| + |\Phi^-\rangle\langle\Phi^-| + |\Psi^+\rangle\langle\Psi^+|)/3$ is also the unique state of the master equation

$$\dot{\rho} = \mathscr{L}_\gamma[S_x]\rho + \mathscr{L}_\gamma[\chi]\rho, \tag{24}$$

where

$$\chi = \begin{bmatrix} 0 & -i \\ 1 & 0 \end{bmatrix} \otimes I + I \otimes \begin{bmatrix} 0 & -i \\ 1 & 0 \end{bmatrix}, \tag{25}$$

corresponding to $\delta\varphi_1 = 0$ and $\delta\varphi_2 = -0.5\pi$. In this sense, the current scheme is robust against the fluctuations of the phases of classical fields, and additionally provides us a simpler method to produce the MDMS in experiment, i.e., only the phase of the driving field coupled to the transition $|e\rangle \leftrightarrow |1\rangle$ needs to be alternatively changed.

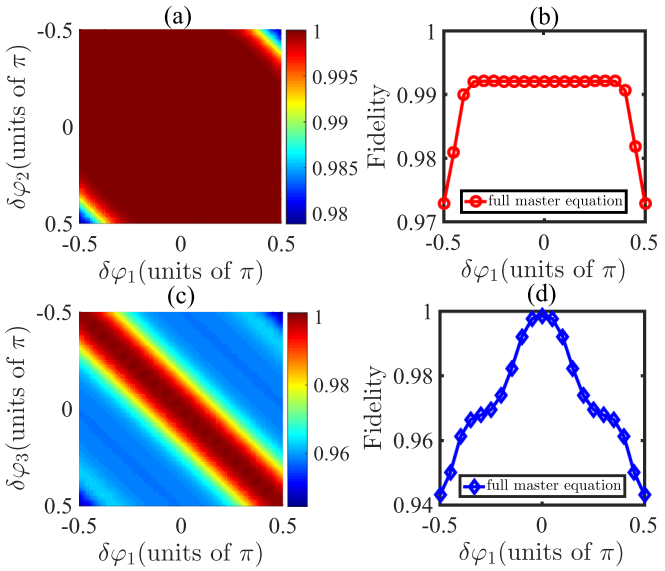

FIG. 10. Phase of aforementioned systems. Panels (a) and (b), respectively, demonstrate how phase mismatch affects the first scheme with effective and full master equations, while panels (c) and (d) show how the phase mismatch influences the second one also with effective and full master equations, respectively. The parameters are taken as (a) $\gamma t = 3$; (b) $\Omega = 0.2g$, $\Delta = 100g$, $N = 40$, and $gt = 12\,000$; (c) $\gamma t = 8$; and (d) $\Omega = 0.5g$, $\Delta = 100g$, and $gt = 8000$, with the initial state $|00\rangle|00\rangle_c$.

As for the coupled-cavity system, since we need four classical fields to individually address two atoms to achieve the collective decay operator S_y, the master equation including the phase mismatch of the corresponding Rabi frequencies reads

$$\dot{\rho}_{m2} = \mathscr{L}_\gamma[ie^{i\delta\varphi_1}|1\rangle_1\langle 0| - ie^{i\delta\varphi_2}|0\rangle_1\langle 1| + ie^{i\delta\varphi_3}|1\rangle_2\langle 0| - ie^{i\delta\varphi_4}|0\rangle_2\langle 1|]\rho + \mathscr{L}_\gamma[S_x]\rho. \tag{26}$$

There are four independent variables $\delta\varphi_i$, which is complicated to discuss. However, if $\delta\varphi_1$ and $\delta\varphi_3$ change synchronously as well as $\delta\varphi_2$ and $\delta\varphi_4$, we can recover the result of Eq. (23). But if $\delta\varphi_1 = \delta\varphi_2$, and $\delta\varphi_3 = \delta\varphi_4$, the uniqueness of the target state is destroyed and makes the scheme sensitive to the mismatch of the phases of classical fields, as shown in Figs. 10(c) and 10(d). Therefore, in this case the phase mismatch $|\delta\varphi|$ should be restricted below 0.1π to promise a high fidelity over 0.99. In other cases, as long as the synchronization of $\delta\varphi_1$ and $\delta\varphi_3$ ($\delta\varphi_2$ and $\delta\varphi_4$) is ruined, the uniqueness of the system's steady state will also be destroyed.

VI. SUMMARY

In summary, our paper has provided two schemes to dissipatively produce the maximally discordant mixed state where the environment becomes a resource for state generation and breaks the time limit of the unitary dynamics. In the first scheme, by alternatively changing the phase of classical fields, the target state turns into the unique steady state of the whole process, while the second one leaves out the alternating

evolutionary process by introducing a lossy coupled-cavity system. We have made a comparison between two schemes. Both of them have advantages and disadvantages. For the first one, it takes a shorter time to achieve the target state with the fidelity oscillated around a certain value. For the second one, although it takes a longer time to achieve the target state, the fidelity is more stable and higher. Meanwhile, both systems have favorable resistance to the spontaneous emission of atoms, and the target state can be obtained with an arbitrary initial state except for the singlet state $|\Psi^-\rangle$. In addition, we have talked over the effect of phase mismatch on the proposed schemes and provided more mathematical forms of the master equation to prepare the MDMS. We have also discussed the relevant parameters under current experimental data and obtained high fidelities over 99%. We hope the paper may be useful for the experimental realization of quantum correlation in the near future.

ACKNOWLEDGMENTS

The authors thank the anonymous reviewers for constructive comments that helped in improving the quality of this paper. This work is supported by the National Natural Science Foundation of China under Grant No. 11774047.

APPENDIX: STEADY-STATE SOLUTION OF EQ. (23)

In order to find the stationary solution of Eq. (23), we are encouraged to expand the density operator ρ in a subspace spanned by

$$|1\rangle = |00\rangle,\ |2\rangle = \frac{1}{\sqrt{2}}(|01\rangle + |10\rangle),\ |3\rangle = |11\rangle. \quad \text{(A1)}$$

Then the effective master equation (23) is changed into

$$\dot{\rho} = \frac{1}{2}\mathscr{L}_\gamma\left[\frac{1}{\sqrt{2}}(-ie^{i\delta\varphi_1}|1\rangle\langle 2| + ie^{i\delta\varphi_2}|2\rangle\langle 1| - ie^{i\delta\varphi_2}|2\rangle\langle 3|\rho + ie^{i\delta\varphi_1}|3\rangle\langle 2|)\right]\rho + \frac{1}{2}\mathscr{L}_\gamma\left[\frac{1}{\sqrt{2}}(|1\rangle\langle 2| + |2\rangle\langle 3|) + \text{H.c.}\right]\rho. \quad \text{(A2)}$$

The steady-state solution of the above equation can be solved by $\dot{\rho} = 0$ and we have

$$\begin{bmatrix} [e^{-i\delta}\rho_{13} + e^{i\delta}\rho_{31} - (4\rho_{11} + \rho_{13} - 4\rho_{22} + \rho_{31})]\gamma & [e^{i\delta}(-2\rho_{21} + \rho_{32}) - (6\rho_{12} - 2\rho_{21} - 4\rho_{23} + \rho_{32})]\gamma & [3\rho_{22} - 4\rho_{13} - 1 - e^{i\delta}(3\rho_{22} - 1)]\gamma \\ [e^{-i\delta}(\rho_{23} - 2\rho_{12}) + 2\rho_{12} - 6\rho_{21} - \rho_{23} + 4\rho_{32}]\gamma & -2(e^{-i\delta}\rho_{13} + e^{i\delta}\rho_{31} + 6\rho_{22} - \rho_{31} - \rho_{13} - 2)\gamma & [e^{i\delta}(\rho_{21} - 2\rho_{32}) + 4\rho_{12} + 2\rho_{32} - \rho_{21} - 6\rho_{23}]\gamma \\ [e^{-i\delta}(1 - 3\rho_{22}) + 3\rho_{22} - 4\rho_{31} - 1]\gamma & [e^{-i\delta}(\rho_{12} - 2\rho_{23}) - \rho_{12} + 4\rho_{21} + 2\rho_{23} - 6\rho_{32}]\gamma & (e^{-i\delta}\rho_{13} + e^{i\delta}\rho_{31} + 4\rho_{11} + 8\rho_{22} - \rho_{13} - \rho_{31} - 4)\gamma \end{bmatrix} = 0, \quad \text{(A3)}$$

where $\delta = \delta\varphi_1 - \delta\varphi_2$. It can be examined both numerically and analytically that Eq. (A3) has a unique steady-state solution except $\delta\varphi_1 = -\delta\varphi_2 = \pm 0.5\pi$.

[1] A. Einstein, B. Podolsky, and N. Rosen, Can quantum-mechanical description of physical reality be considered complete? Phys. Rev. **47**, 777 (1935).
[2] A. K. Ekert, Quantum Cryptography Based on Bell's Theorem, Phys. Rev. Lett. **67**, 661 (1991).
[3] C. H. Bennett and S. J. Wiesner, Communication via One- and Two-Particle Operators on Einstein-Podolsky-Rosen States, Phys. Rev. Lett. **69**, 2881 (1992).
[4] C. H. Bennett, G. Brassard, C. Crépeau, R. Jozsa, A. Peres, and W. K. Wootters, Teleporting an Unknown Quantum State via Dual Classical and Einstein-Podolsky-Rosen Channels, Phys. Rev. Lett. **70**, 1895 (1993).
[5] P. Walther, K. J. Resch, T. Rudolph, E. Schenck, H. Weinfurter, V. Vedral, M. Aspelmeyer, and A. Zeilinger, Experimental one-way quantum computing, Nature (London) **434**, 169 (2005).
[6] R. F. Werner, Quantum states with Einstein-Podolsky-Rosen correlations admitting a hidden-variable model, Phys. Rev. A **40**, 4277 (1989).
[7] D. W. Lyons, A. M. Skelton, and S. N. Walck, Werner state structure and entanglement classification, Adv. Math. Phys. **2012**, 463610 (2012).
[8] H. Ollivier and W. H. Zurek, Quantum Discord: A Measure of the Quantumness of Correlations, Phys. Rev. Lett. **88**, 017901 (2001).
[9] K. Modi, A. Brodutch, H. Cable, T. Paterek, and V. Vedral, The classical-quantum boundary for correlations: Discord and related measures, Rev. Mod. Phys. **84**, 1655 (2012).
[10] J. Yune, K.-H. Hong, H.-T. Lim, J.-C. Lee, O. Kwon, S.-W. Han, Y.-S. Kim, S. Moon, and Y.-H. Kim, Quantum discord protection from amplitude damping decoherence, Opt. Express **23**, 26012 (2015).
[11] M. Gu, H. M. Chrzanowski, S. M. Assad, T. Symul, K. Modi, T. C. Ralph, V. Vedral, and P. K. Lam, Observing the operational significance of discord consumption, Nat. Phys. **8**, 671 (2012).
[12] F. Galve, G. L. Giorgi, and R. Zambrini, Maximally discordant mixed states of two qubits, Phys. Rev. A **83**, 012102 (2011).
[13] C. E. López, F. Albarrán-Arriagada, S. Allende, and J. C. Retamal, Generation of maximally correlated states of $(d \otimes d)$-dimensional systems in the absence of entanglement, Europhys. Lett. **120**, 10003 (2017).
[14] M. B. Plenio, S. F. Huelga, A. Beige, and P. L. Knight, Cavity-loss-induced generation of entangled atoms, Phys. Rev. A **59**, 2468 (1999).
[15] M. B. Plenio and S. F. Huelga, Entangled Light from White Noise, Phys. Rev. Lett. **88**, 197901 (2002).
[16] G. Vacanti and A. Beige, Cooling atoms into entangled states, New. J. Phys. **11**, 083008 (2009).

[17] M. J. Kastoryano, F. Reiter, and A. S. Sørensen, Dissipative Preparation of Entanglement in Optical Cavities, Phys. Rev. Lett. **106**, 090502 (2011).

[18] Y. Lin, J. P. Gaebler, F. Reiter, T. R. Tan, R. Bowler, A. S. Sørensen, D. Leibfried, and D. J. Wineland, Dissipative production of a maximally entangled steady state of two quantum bits, Nature (London) **504**, 415 (2013).

[19] A. W. Carr and M. Saffman, Preparation of Entangled and Antiferromagnetic States by Dissipative Rydberg Pumping, Phys. Rev. Lett. **111**, 033607 (2013).

[20] X.-Q. Shao, T.-Yu. Zheng, C. H. Oh, and S. Zhang, Dissipative creation of three-dimensional entangled state in optical cavity via spontaneous emission, Phys. Rev. A **89**, 012319 (2014).

[21] L.-T. Shen, R.-X. Chen, Z.-B. Yang, H.-Z. Wu, and S.-B. Zheng, Preparation of two-qubit steady entanglement through driving a single qubit, Opt. Lett. **39**, 6046 (2014).

[22] X. Q. Shao, J. H. Wu, and X. X. Yi, Dissipation-based entanglement via quantum Zeno dynamics and Rydberg antiblockade, Phys. Rev. A **95**, 062339 (2017).

[23] X.-Q. Shao, Engineering steady entanglement for trapped ions at finite temperature by dissipation, Phys. Rev. A **98**, 042310 (2018).

[24] D. X. Li and X. Q. Shao, Unconventional Rydberg pumping and applications in quantum information processing, Phys. Rev. A **98**, 062338 (2018).

[25] D. X. Li and X. Q. Shao, Directional quantum state transfer in a dissipative Rydberg-atom-cavity system, Phys. Rev. A **99**, 032348 (2019).

[26] S.-L. Su, X.-Q. Shao, H.-F. Wang, and S. Zhang, Scheme for entanglement generation in an atom-cavity system via dissipation, Phys. Rev. A **90**, 054302 (2014).

[27] S.-L. Su, Q. Guo, H.-F. Wang, and S. Zhang, Simplified scheme for entanglement preparation with Rydberg pumping via dissipation, Phys. Rev. A **92**, 022328 (2015).

[28] W. Qin, A. Miranowicz, P.-B. Li, X.-Y. Lü, J. Q. You, and F. Nori, Exponentially Enhanced Light-Matter Interaction, Cooperativities, and Steady-State Entanglement Using Parametric Amplification, Phys. Rev. Lett. **120**, 093601 (2018).

[29] Y.-H. Chen, Z.-C. Shi, J. Song, Y. Xia, and S.-B. Zheng, Accelerated and noise-resistant generation of high-fidelity steady-state entanglement with Rydberg atoms, Phys. Rev. A **97**, 032328 (2018).

[30] C. Yang, D. X. Li, and X. Q. Shao, Dissipative preparation of Bell states with parallel quantum Zeno dynamics, Sci. China Phys. Mech. Astronomy **62**, 110312 (2019).

[31] E. G. Dalla Torre, J. Otterbach, E. Demler, V. Vuletic, and M. D. Lukin, Dissipative Preparation of Spin Squeezed Atomic Ensembles in a Steady State, Phys. Rev. Lett. **110**, 120402 (2013).

[32] M. Ali, A. R. P. Rau, and G. Alber, Quantum discord for two-qubit x states, Phys. Rev. A **81**, 042105 (2010).

[33] K.-J. Engel and R. Nagel, *One-Parameter Semigroups for Linear Evolution Equations* (Springer, New York, 2000).

[34] M. A. Nilsen and I. L. Chuang, *Quantum Computation and Quantum Information* (Cambridge University, Cambridge, England, 2000).

[35] Z.-H. Chen, Z. Ma, F.-L. Zhang, and J.-L. Chen, Super fidelity and related metrics, Cent. Eur. J. Phys. **9**, 1036 (2011).

[36] V. Vedral, M. B. Plenio, M. A. Rippin, and P. L. Knight, Quantifying Entanglement, Phys. Rev. Lett. **78**, 2275 (1997).

[37] V. Vedral and M. B. Plenio, Entanglement measures and purification procedures, Phys. Rev. A **57**, 1619 (1998).

[38] R. L. Kosut, A. Shabani, and D. A. Lidar, Robust Quantum Error Correction via Convex Optimization, Phys. Rev. Lett. **100**, 020502 (2008).

[39] P. Giorda and P. Zanardi, Quantum chaos and operator fidelity metric, Phys. Rev. E **81**, 017203 (2010).

[40] J. A. Miszczak, Z. Puchala, P. Horodecki, A. Uhlmann, and K. Zyczkowski, Sub- and super-fidelity as bounds for quantum fidelity, Quantum Inf. Comput. **9**, 103 (2009).

[41] W. K. Wootters, Entanglement of formation and concurrence, Quantum Inf. Comput. **1**, 27 (2001).

[42] F. Altintas, A. Kurt, and R. Eryigit, Classical memoryless noise-induced maximally discordant mixed separable steady states, Phys. Lett. A **377**, 53 (2012).

[43] E. K. Irish, C. D. Ogden, and M. S. Kim, Polaritonic characteristics of insulator and superfluid states in a coupled-cavity array, Phys. Rev. A **77**, 033801 (2008).

[44] J. Cho, D. G. Angelakis, and S. Bose, Fractional Quantum Hall State in Coupled Cavities, Phys. Rev. Lett. **101**, 246809 (2008).

[45] T. C. H. Liew and V. Savona, Multimode entanglement in coupled cavity arrays, New J. Phys. **15**, 025015 (2013).

[46] M. Hartmann, F. G. S. L. Brandão, and M. Plenio, Quantum many-body phenomena in coupled cavity arrays, Laser Photonics Rev. **2**, 527 (2008).

[47] A. Serafini, S. Mancini, and S. Bose, Distributed Quantum Computation via Optical Fibers, Phys. Rev. Lett. **96**, 010503 (2006).

[48] F. Brennecke, T. Donner, S. Ritter, T. Bourdel, M. Köhl, and T. Esslinger, Cavity QED with a Bose-Einstein condensate, Nature (London) **450**, 268 (2007).

[49] C. Guerlin, E. Brion, T. Esslinger, and K. Mølmer, Cavity quantum electrodynamics with a Rydberg-blocked atomic ensemble, Phys. Rev. A **82**, 053832 (2010).

[50] X.-F. Zhang, Q. Sun, Yu.-C. Wen, W.-M. Liu, S. Eggert, and A.-C. Ji, Rydberg Polaritons in a Cavity: A Superradiant Solid, Phys. Rev. Lett. **110**, 090402 (2013).

[51] A. Grankin, E. Brion, E. Bimbard, R. Boddeda, I. Usmani, A. Ourjoumtsev, and P. Grangier, Quantum statistics of light transmitted through an intracavity Rydberg medium, New J. Phys. **16**, 043020 (2014).

[52] S. M. Spillane, T. J. Kippenberg, K. J. Vahala, K. W. Goh, E. Wilcut, and H. J. Kimble, Ultrahigh-q toroidal microresonators for cavity quantum electrodynamics, Phys. Rev. A **71**, 013817 (2005).

[53] B. Dayan, A. S. Parkins, T. Aoki, E. P. Ostby, K. J. Vahala, and H. J. Kimble, A photon turnstile dynamically regulated by one atom, Science **319**, 1062 (2008).